IEEE Access
Multidisciplinary | Rapid Review | Open Access Journal

Date of publication xxxx 00, 0000, date of current version xxxx 00, 0000.

Digital Object Identifier 10.1109/ACCESS.2020.XXXX

A Methodology to Characterize Power Control Systems for Limiting Exposure to Electromagnetic Fields generated by Massive MIMO Antennas

SARA ADDA[1], TOMMASO AURELI[2], STEFANO COLTELLACCI[2], STEFANO D'ELIA[3], DANIELE FRANCI[2], ENRICO GRILLO[2], NICOLA PASQUINO[4], (Senior Member, IEEE), SETTIMIO PAVONCELLO[2], RICCARDO SUMAN[3], and MATTIA VACCARONO.[1]

[1]Arpa Piemonte, Dipartimento Rischi Fisici e Tecnologici, Ivrea (TO) 10015 ITALY (email: sara.adda@arpa.piemonte.it; mattia.vaccarono@arpa.piemonte.it)
[2]2ARPA Lazio (Agenzia per la Protezione Ambientale del Lazio), Rome, 00172 ITALY (email: tommaso.aureli@arpalazio.gov.it; stefano.coltellacci@arpalazio.gov.it; daniele.franci@arpalazio.gov.it; enrico.grillo@arpalazio.gov.it; settimio.pavoncello@arpalazio.gov.it)
[3]Vodafone Italia SpA, Group Network, Mobile Access Engineering, Ivrea (TO) 10015 ITALY (email: stefano.delia@vodafone.com; riccardo.suman@vodafone.com)
[4]Dipartimento di Ingegneria Elettrica e delle Tecnologie dell'Informazione, Università degli Studi di Napoli Federico II, Napoli, Italy (email: nicola.pasquino@unina.it)

Corresponding author: Nicola Pasquino (e-mail: nicola.pasquino@unina.it).

ABSTRACT The fifth-generation (5G) New Radio (NR) cellular network has been launched recently. The assignment of new spectrum bands and the widespread use of Massive MIMO (MaMIMO) and beamforming techniques for better radio coverage are two major features of the new architecture. They imply both opportunities and challenges, one of the most daring one among the latter ones is the research for methods to assess human exposure to electromagnetic fields radiated by the base stations. The long-term time-varying behavior and spatial multiplexing feature of the MaMIMO antennas, along with the radio resource utilization and adoption of Time-Division Duplexing (TDD), requires that the assessment of exposure to electromagnetic fields radiated by 5G systems is based on a statistical approach that relies on the space and time distribution of the radiated power. That, in turn, is determined through simulations based on the actual maximum transmitted power – defined as the 95th percentile of the empirical distribution obtained from historical data of radiated power – rather than on the nominal one. To ensure that exposure limits are never exceeded, a monitoring and control system (usually referred to as Power Lock (PL)) that limits the transmitted power can be used. In this paper we propose a methodology, independent from the specific technical solution implemented by the manufacturer, to characterize such control systems and determine their capability to limit the average power transmitted over a given time interval to a value that keeps the corresponding average exposure to electromagnetic fields below a specified value. Experimental results show the effectiveness of the methodology and that it can also be used to identify when the PL interacts with the higher levels of the MaMIMO system architecture.

INDEX TERMS radio frequency electromagnetic fields, exposure assessment, Massive MIMO, 5G, New Radio, measurements, mobile telecommunications, channel power.

I. INTRODUCTION

THE fifth-generation (5G) New Radio (NR) system is being rolled out over the world and is expected to provide a solid commercial service within the next few years. Expectations about its performance are high mostly because of the dramatic change in the paradigm of cellular network that it carries along [1]–[5].

Beside signal protocol and network architecture, a major difference with previous-generation mobile systems is the radio interface. Unlike traditional systems that use passive antennas whose radiation pattern is static over time, the NR system uses Massive MIMO (MaMIMO) [6]–[9] technology where active antennas, with different configurations [10,11], are used to generate multiple radiation lobes with power

This article has been accepted for publication in a future issue of this journal, but has not been fully edited. Content may change prior to final publication. Citation information: DOI 10.1109/ACCESS.2020.3024764, IEEE Access

and shape variable over time, obtained with beamforming techniques [12].

The radiation pattern and gain of an antenna, together with the input power and the characteristics of the propagation channel, determine the distribution of the electromagnetic field (EMF) in the space surrounding the radiant system. For MaMIMO antenna there is no direct proportionality between the total transmitted power and the Equivalent Isotropic Radiated Power (EIRP) along the user's direction. It follows that the evaluation of its total transmitted power does not allow for a deterministic assessment of the actual distribution of the electromagnetic field strength in the space and over time.

Assessment of the exposure to electromagnetic fields, therefore, requires a statistical approach that relies on the space and time distribution of the radiated power [13,14], as indicated in the standard IEC 62232 [15] and the technical report IEC TR 62669 [16], through numerical methods based on the *actual maximum transmitted power* (defined as the 95$^{\text{th}}$ percentile of the empirical distribution obtained from historical data of radiated power) approach. The operator shall, therefore, ensure that the actual maximum transmitted power threshold is not exceeded during service. This can be done using counters or tools to monitor the transmitted power or EIRP.

When the actual maximum transmitted power approach is implemented through counters, the operator shall collect and monitor data from radio counters to make sure that the transmitted power, averaged over a time interval corresponding to the averaging time of the applicable exposure limits (typically 6 [17] or 30 min [18]), are maintained below the maximum allowed threshold. The International Electrotechnical Commission (IEC) [15,16] allows that, over a limited time, the cell may exceed the conservative value for at most 5% of the measured values [19], provided that the EMF average exposure keeps below the limit. IEC also describes a control feature based on network counters which can be used to check that the power threshold is never exceeded when averaging over time.

Alternatively, the operators can activate automatic tools to monitor and control the transmitted power (or EIRP) of a MaMIMO antenna to ensure that the threshold values configured for each MaMIMO antenna are not exceeded, as described in [20]. Such tools are usually referred to as Power Lock (PL) features, and their main operational characteristics will be described in Sect. II.

This paper presents a methodology to test the functionalities of a power control and limitation system. The main purpose of the methodology is to verify that such power lock feature meets the requirement of limiting the transmitted power of the traffic channel only, without acting on the control channel. It is organized as follows: after detailing the main functional characteristics of the PL in Sect. II, an overview of the 5G NR grid structure is provided in Sect. III, the proposed methodology and the measurement setup for its validation are presented in Sect. IV and V, respectively. Experimental results are reported and commented in Sect. VI, while conclusions are drawn in Sect. VII.

II. POWER LOCK FUNCTIONAL DESCRIPTION

Documents [15,16] by IEC and [20] by the Next Generation Mobile Networks (NGMN) Alliance do not provide any details about the implementation of the PL feature for controlling and limiting the radio frequency (RF) transmitted power, because it is considered a specific task to be performed by the radio equipment manufacturer. Given that the latter is unlikely to provide detailed information about how such feature works in its own implementation, this section presents a description of the principles of the main PL functionalities, enriched by the information acquired during the test session.

The PL has to monitor the power transmitted by the MaMIMO system at a very high rate (possibly once in each transmission time interval (TTI) or every few milliseconds at most) and automatically limit the maximum value so that the average transmitted power over a reference time interval does not exceed the allowed threshold. Practically, for, say, every TTI the feature has to monitor the RF output power of every transceiver module (TRx), which then feeds the MaMIMO antenna, typically made of an array of dipoles so that every TRx might be connected to one or more of them. Moreover, the RF power is in a direct relationship with the transmitted EIRP through the antenna gain. Therefore, knowing the maximum antenna array gain, the radiated power can be monitored in each TTI and, in turn, the average power transmitted in a given interval (e.g., 6 min) can be obtained.

The purpose of the PL is not simply to calculate the average transmitted power, which task is performed by specific counters for measuring the key performance indicators (KPIs) of the network. Instead, its goal is to ensure that the average transmitted power over the assigned time interval does not exceed the allowed threshold, so the PL has to establish when and how to limit the maximum power that can be transmitted by the MaMIMO antenna in the remaining portion of the reference time interval based on the average power transmitted in the initial portion of the interval.

For example, assuming that the instantaneous maximum power P_{max} is initially set at 100 W and the threshold for the average power over 6 min at 25 W (25% of P_{max}), if for the first minute the average transmitted power is equal to P_{max} (i.e., the antenna constantly transmits at P_{max}), then for the remaining 5 min P_{max} will be reduced to 10 W, so that the average power over the whole 6 min will be $P_{\text{avg}} = (1 \cdot 100 + 5 \cdot 10)/6 = 25\,\text{W}$. As a consolidated practice adopted by all manufacturers to all technologies, the maximum instantaneous power P_{max} that can be transmitted is tuned through the Operational Service System (OSS) in the baseband unit (BBU) of the MaMIMO antenna, the maximum power amplifier output being its upper bound.

In the tested system the amount of power reduction is

fixed, that is the PL does not calculate it and sets it to the average threshold. In other words, when the feature is activated the maximum instantaneous power that the MaMIMO antenna can transmit is either equal to the maximum power or to the power threshold. Referring to the previous example, the maximum power that can be transmitted is, therefore, either equal to 100 W when the PL is inactive or 25 W when the PL is operating. As a result, in the case that the MaMIMO antenna starts transmitting at 100 W, in order to ensure that the average power is equal to 25 W, the feature should reduce immediately the maximum transmitted power down to 25 W.

As said before, the implementation of the feature is completely up to the manufacturer (and, as such, patented), especially with reference to when the PL activates and how it reduces the RF power. The only piece of information that was disclosed to the Authors is that the PL interacts with the downlink scheduler to dynamically reduce the momentary output power by decreasing the power of the Physical Downlink Shared Channel (PDSCH) and/or reducing the assigned Resource Blocks (RBs). Moreover, the feature ensures that no change in the NR coverage is experienced by users by operating only on traffic channels, not on control channels.

It must be said, however, that decreasing the power of the traffic channels or reducing the number of RBs assigned to a user could lead to a degradation of the quality and performance experienced by the users when the system is operated in high traffic conditions.

III. 5G NEW RADIO (NR) GRID STRUCTURE

In this section, we present the key principles of the physical layer of 5G NR that are important for RF exposure assessment [21]. The 5G NR frame structure is shown in Fig. 1. It relies on Orthogonal Frequency-Division Multiplexing (OFDM) and supports operation in the spectrum ranging from sub-1 GHz to millimeter-wave bands. Two frequency ranges (FRs) are defined in the 3rd Generation Partnership Project (3GPP) technical specifications [22]–[24]:

- FR1: 450 MHz to 7.125 GHz, commonly referred to as sub-6 GHz;
- RF2: 24.25 GHz to 52.6 GHz, commonly referred to as millimeter waves.

With the purpose of ensuring the 5G NR and LTE coexistence on the same frequency band, the time length of the 5G NR frame is 10 ms and consists of 10 subframes, each having a time length of 1 ms, as in the LTE system. Unlike the LTE, 5G NR uses a *flexible numerology* characterized by the parameter μ [23]. The *flexible numerology* allows 5G NR to provide a wide range of services requiring different latency and capacity, offering the possibility to manage low latency services instead of only high data transmission applications [25]. Moreover, as an additional difference with the LTE, 5G NR allows simultaneous multi-numerology utilization. The 5G NR multi-numerology structures was also studied in [26]–[31], whereas one of the first studies on a framework that provides several different services simultaneously in a unified framework applying the multi-numerology paradigm was [25].

In the 5G NR frame structure, each subframe consists of 2^{μ} time slots, in order to cope with the wide range of applications for which it was designed and the large spectrum availability. Each slot of $1/2^{\mu}$ ms contains 14 OFDM symbols (12 OFDM symbols in case of extended cyclic prefix). Accordingly, each symbol duration is equal to $(14 \cdot 2^{\mu})^{-1}$ ms ($(12 \cdot 2^{\mu})^{-1}$ ms for extended prefix). Therefore, the number of symbols contained in each subframe depends on the value of μ: larger values of μ allow for more symbols in the same subframe.

Different numerologies are associated to different OFDM subcarrier distances. In particular, the subcarrier spacing is $2^{\mu} \cdot 15$ kHz, with $\mu = \{0, 1, 2, 3, 4\}$. Subcarrier spacing of 15 kHz, 30 kHz and 60 kHz are used in sub-6 GHz band (FR1), while 60 kHz and 120 kHz are used for millimeter-wave band (FR2). Instead, the 240 kHz spacing is reserved for non-data (signaling) channels. Note that for $\mu = 0$ NR uses the same spacing of the LTE subcarrier (15 kHz), thus ensuring full compatibility between the two systems on the same frequency band. An NR carrier is made of up to 3276 subcarriers. The maximum bandwidth of each NR carrier is 100 MHz for sub-6 GHz band (FR1) and 400 MHz for millimeter-wave band (FR2). Both values are much greater than the LTE bandwidth, which is limited to 20 MHz. In order to manage different numerologies simultaneously, in 5G NR the Bandwidth Part (BWP) has been introduced, which consists of a group of contiguous Physical Resource Blocks (PRBs) defining a fixed portion of the frequency band over which the communication takes place with a given numerology [24]. Each BWP has its own numerology that fixes the cyclic prefix length and the subcarrier spacing. Furthermore, unlike the LTE, since 5G User Equipments (UEs) need to monitor only the assigned BWPs, they don't need to scan the whole bandwidth, thus reducing the UE's power consumption. The Resource Grid (RG) [23] is a time-frequency representation of the radio resources available for transmission. RG is characterized by one subframe in the time domain and full carrier bandwidth in the frequency domain (see Fig. 1). Since 5G NR supports different numerologies, there is a different RG extension for each of them. The smallest unit of the RG is represented by one subcarrier in the frequency domain observed for the time duration of one OFDM symbol, named Resource Element (RE). REs are grouped into PRBs consisting of 12 consecutive subcarriers in the frequency domain.

Analyzing the RG is extremely complex, and the reader is referred to [23] for a thorough discussion about it. Nonetheless, since detection and decoding of the Control and Synchronization signals is particularly useful and interesting for the assessment of exposure, in the following we describe those signals briefly. In 5G, Synchronization Signal and Physical Broadcast Channel (PBCH) are packed as a single block (Fig. 2). More specifically, the Synchroniza-

This article has been accepted for publication in a future issue of this journal, but has not been fully edited. Content may change prior to final publication. Citation information: DOI 10.1109/ACCESS.2020.3024764, IEEE Access

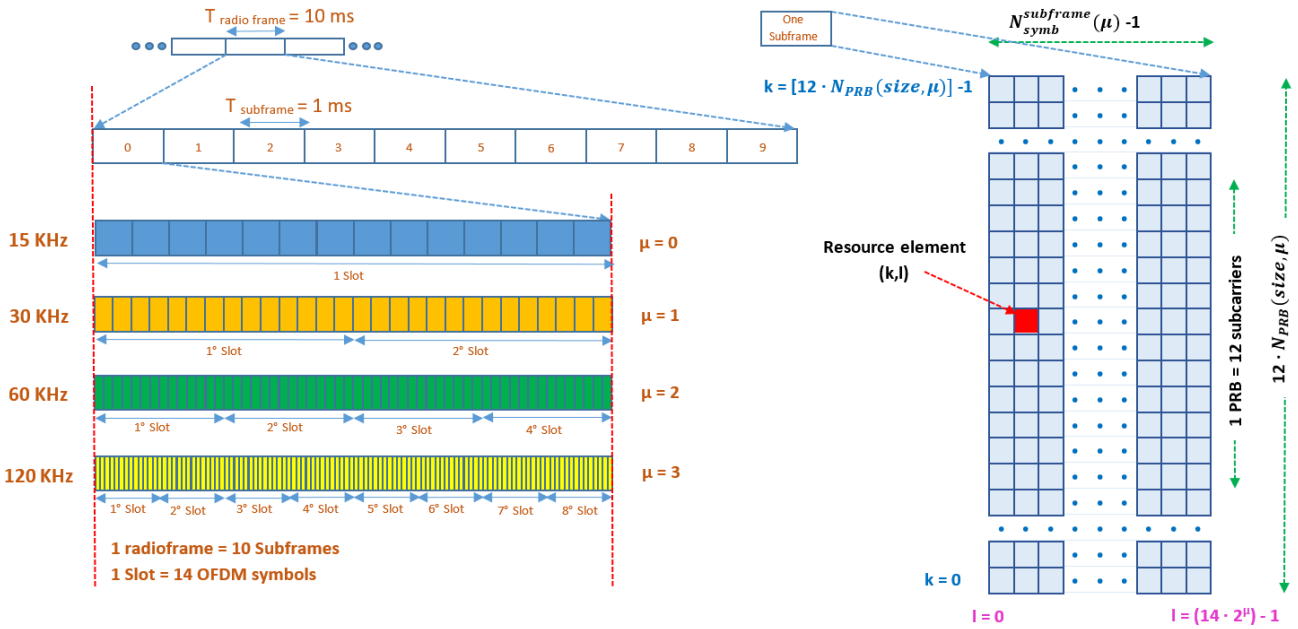

Figure 1. 5G NR frame structure and resource grid basic terminology.

tion Signal/Physical Broadcast Channel (SS/PBCH), also named Synchronization Signal Block (SSB), occupies 240 contiguous subcarriers and four contiguous OFDM symbols. It contains four different types of signals: the Primary Synchronization Signal (PSS), the Secondary Synchronization Signal (SSS), the PBCH and the PBCH Demodulation Reference Signal (PBCH-DMRS). SSBs are grouped in blocks named SSB bursts (see Fig. 2), transmitted in the first 5 ms of the frame, with a configurable periodicity of 5, 10, 20, 40, 80 or 160 ms. Block patterns are a function of the FR and subcarriers spacing, and the 3GPP technical specification (see [24, §4 Synchronization Procedures]) defines five different cases (i.e., A, B, C, D, E) for a total of eight possible configurations.

The maximum number of SSBs in a single burst is indicated with $L_{\max}$ and ranges from 4 or 8 for cases A, B and C (FR1) to 64 in cases D and E (FR2). SSBs grouped in an SSB burst are used to implement initial UE radio access and are involved in the *beam sweeping* procedure. Each SSB is associated to a different beam which points to a different direction in the space. The UE, during the initial radio access setup, locks to the beam that provides the strongest received signal (see Fig. 3).

IV. PROPOSED METHODOLOGY

Since it is unlikely that a radio equipment manufacturer provides detailed information about how the power monitoring and controlling feature – hereafter named Power Lock (PL) – is implemented, and how it interacts with the downlink scheduler in order to dynamically reduce the instantaneous transmitted power, the proposed methodology is focused on the assessment of the PL's capability to ensure that the EMF exposure complies with limits, usually set as the average over a given time interval. Moreover, the methodology is independent of the specific technical solution and implementation of the PL and can, therefore, be applied to any commercial and experimental solution without loss of generality. As a matter of fact, it is based on a black-box approach consisting of a simple measurements procedure that, furthermore, can be easily replicated during the whole MaMIMO antenna's life cycle to check that the PL maintains its designed operational features over time.

To better understand the methodology, it is useful to introduce the main quantities that we will refer to:

- P_t is the *instantaneous* power transmitted by the MaMIMO system;
- $P_{\max}$ is the *maximum instantaneous* power that can be transmitted by the MaMIMO system at any time (i.e., the upper bound of P_t, so that $P_{\max} \geq P_t$);
- $\mathrm{F_{TDC}}$ is the *Technology Duty Cycle Factor*, a deterministic scaling factor representing the fraction of the signal frame reserved to the downlink transmission [16];
- $P_{\mathrm{avg,max}}$ is the *maximum average* power that can be transmitted by the MaMIMO system over a time interval τ of duration 6 min [17] or 30 min [18]. If PL is inactive and P_t is constant and equal to $P_{\max}$, then $P_{\mathrm{avg,max}} = P_{\max} - |\mathrm{F_{TDC}}|$, whereas if PL is active, there is no such relation because its value is imposed by PL;
- E_0 is the *maximum average* EMF exposure over τ allowed for the specific MaMIMO system on which the PL is tested. E_0 is set according to the

This article has been accepted for publication in a future issue of this journal, but has not been fully edited. Content may change prior to final publication. Citation information: DOI 10.1109/ACCESS.2020.3024764, IEEE Access

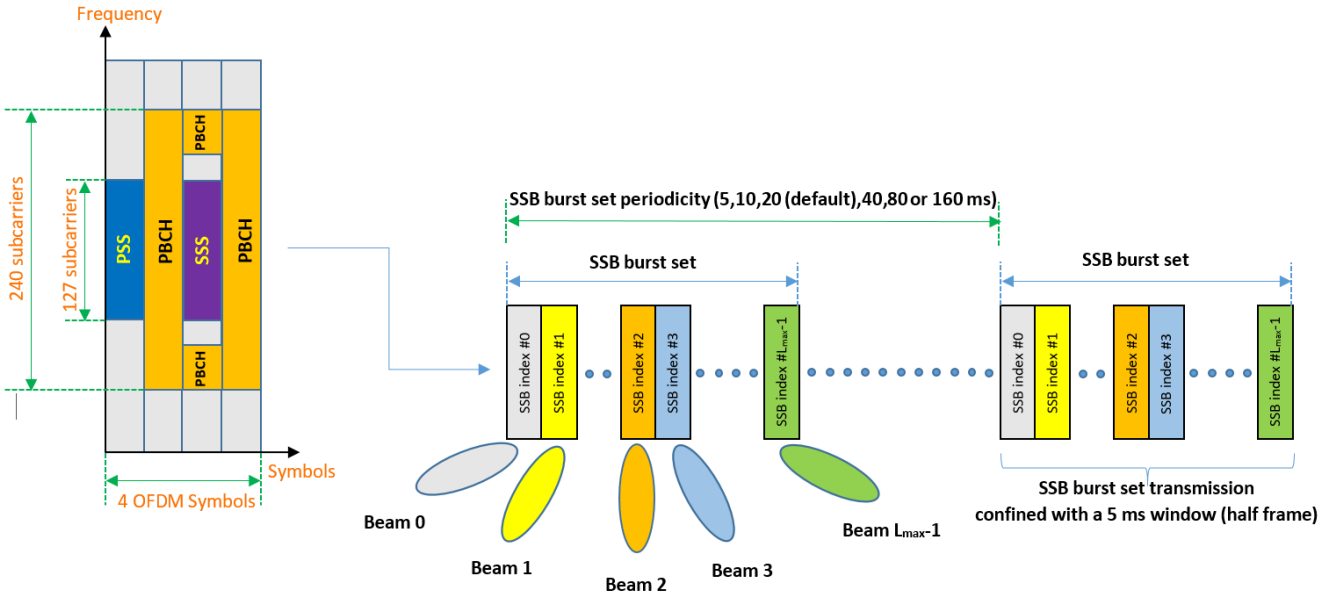

Figure 2. 5G NR Synchronization Signal Block (SSB) definition and burst structure.

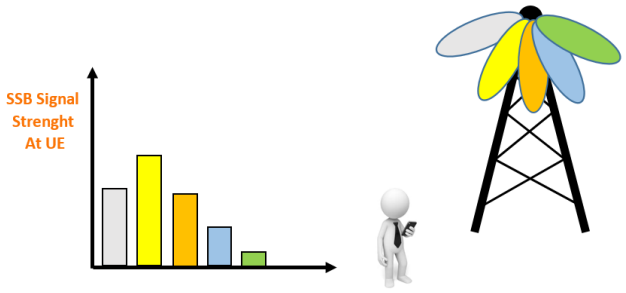

Figure 3. 5G NR beam sweeping.

radiation-protection legislation under the condition of simultaneous exposure to high-frequency EMF fields generated by all the systems installed at the same site or at nearby sites and supposing that the effects of exposures are additive;

P_0 is the *maximum average* power that results in an exposure equal to E_0 over τ.

For a proper assessment of the PL operating characteristics, the methodology requires that P_t is equal to the maximum allowed power at all times during the validation procedure, which in turns implies that the full downlink capacity of the MaMIMO antenna under test is deployed. To operate under such conditions, one or more UEs capable of forcing high data-rate download transmission are required. Indeed, if such condition is not met the PL may possibly never activate because the average power may never reach the maximum allowed average value P_0.

The performance assessment of the PL can be run through the methodology described in the following:

1) *Fixing of* P_0. It is first required that P_0 is fixed through a numerical or experimental approach that leads to determining the constant power P_t that results in an average EMF exposure over τ equal to E_0. During this operation, the PL is off, which condition will be labeled as PL_{off}, and it is imposed that $P_{\text{avg,max}} = P_0$. In fact, to make sure that EMF exposure during normal operation of a MaMIMO system without PL is compliant with the limits, $P_{\text{avg,max}}$ can be at most equal to the power P_0 that results in an exposure equal to E_0. We observe that at the end of this step also the value of P_{max} is determined: $P_{\text{max}} = P_0 + |\text{F}_{\text{TDC}}|$.
As introduced in Sect. II, the (maximum) instantaneous power P_t (P_{max}) that can be transmitted is set through the OSS in the BBU of the MaMIMO antenna.
2) *Increase of* P_{max}. P_{max} is increased by an amount ΔP and, since $P_{\text{avg,max}}$ is a known and fixed portion of P_{max} when PL is off, $P_{\text{avg,max}}$ is also increased by the same amount: $P_{\text{avg,max}} = P_0 + \Delta P$. Similarly to step 1, P_{max} has been increased by operating on the OSS in the BBU of the MaMIMO antenna.
To confirm that the MaMIMO system has been correctly configured with the new P_{max}, the average EMF exposure over τ is measured: the resulting EMF strength should increase by the same amount ΔP. Furthermore, since PL is off, both traffic and control channels strength should increase.
3) *Activation and validation of PL.* With the increased value of P_{max}, PL is activated (i.e., PL_{on}) and configured to limit the average power transmitted over τ to P_0. This means that P_t will gradually decrease from the initial value P_{max} so that its average value over τ

This article has been accepted for publication in a future issue of this journal, but has not been fully edited. Content may change prior to final publication. Citation information: DOI 10.1109/ACCESS.2020.3024764, IEEE Access

Figure 4. Overview of the measurement site.

is equal to P_0.

Measurements of the EMF exposure will give evidence that its average value is compliant with E_0 and that PL only affects traffic channels while having control channel transmitted at the maximum power $P_{\max}$.

The experimental activity to validate the proposed methodology requires a different test for each step described above. To change the system configuration, tests must be interleaved with *idle* time intervals during which only control channels are active to keep the system alive and reachable by the UEs.

Before proceeding with the presentation of the measurement setup and discussion of the experimental results, we wish to stress, once again, that our proposal refers to a methodology to assess the performance of a PL feature, i.e., its capability to reduce the radiated power to maintain exposure to EMF below the applicable limits. As such, the measurement of EMF exposure itself is not the focus of this paper, neither are we proposing a method for a better assessment of exposure levels. As a matter of fact, as explained above, EMF strength measurements only come into play to verify the effectiveness of the PL's action. For that specific task, we used the procedure detailed in [32], although we are aware that the issues and challenges related to EMF measurements in 5G technology are wide and still open, as testified by the increasing number of papers focusing on them (see [21,32]–[36] as an example).

V. MEASUREMENT SETUP

The proposed exposure assessment methodology was validated in a Line-of-Sight (LOS) environment in the city of Rome, Italy (see. Fig. 4) using a commercial Time-Division Duplexing (TDD) 3.5 GHz MaMIMO antenna system manufactured by Huawei. The main characteristics of the transmitted 5G signal are reported in Tab. 1 and Fig. 5, while a summary of the tests used in the experimental campaign reported in Sect. VI to validate the methodology is listed in Tab. 2.

Three different measurement chains were used for the validation:

Table 1. 5G signal configuration.

Antenna	MaMIMO 64T64R
Center frequency f_c	3680.01 MHz
Bandwidth	80 MHz
Duplexing	TDD
Frame configuration	8 : 2
Subcarrier spacing	30 kHz
F_{TDC}	−1.3 dB
μ	1
Symbol duration	33.3 µs
Cyclic Prefix (CPr) duration	4.7 µs
slots/frame	20
slots/subframe	2
symbols/slot	14
SSB center frequency	3649.44 MHz
SSB configuration	Case C
SSBs per burst	6

Table 2. Test configuration.

Test no.	Power Lock	$P_{\max}$	$P_{\text{avg,max}}$	F_{TDC}
1	OFF	46 dBm	44.7 dBm	−1.3 dB
2	OFF	51 dBm	49.7 dBm	−1.3 dB
3	ON	51 dBm	44.7 dBm	−1.3 dB

1) A Rohde & Schwarz (R&S) FSP30 spectrum analyzer connected to a Keysight N6850A broadband omnidirectional antenna, remotely controlled by a custom software acquisition tool developed by ARPA Lazio, was used to measure the Channel Power (CP). The configuration is shown in Tab. 3.
2) A Narda SRM3006 field strength analyzer equipped with a Narda 3502/01 isotropic antenna was used in Zero Span mode to measure the EMF strength. The configuration is shown in Tab. 4.

   Given that there is no specific standard for this kind of measurements, we wish to highlight the rationale for the choice of the parameters. The center frequency $f_c = 3649.44$ MHz is different from that of the 5G signal ($f_c = 3680.01$ MHz) to detect the SSBs:

Table 3. Channel Power measurement configuration.

Center frequency f_c	3680.01 MHz
Integration Bandwidth (IB)	80 MHz
Resolution Bandwidth (RBW)	100 kHz
Video Bandwidth (VBW)	300 kHz
Sweep Time (SWT)	100 ms
Trace	Average ($n = 200$)
Detector	RMS
Trigger	continuous

This article has been accepted for publication in a future issue of this journal, but has not been fully edited. Content may change prior to final publication. Citation information: DOI 10.1109/ACCESS.2020.3024764, IEEE Access

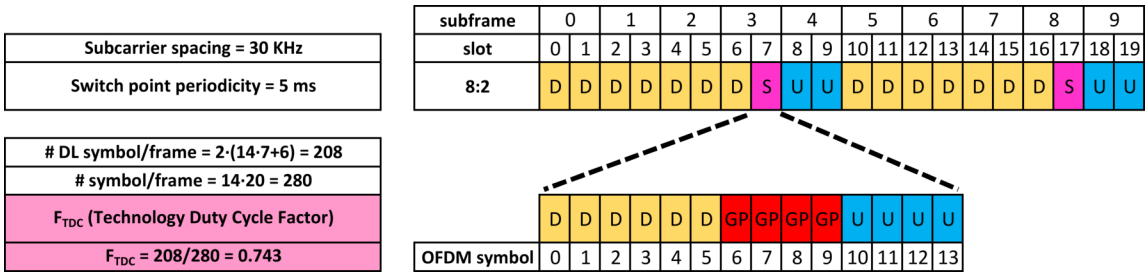

Figure 5. Technology Duty Cycle Factor (F_{TDC}).

Table 4. Zero Span field strength measurement configuration.

Center frequency f_c	3649.44 MHz
RBW	2 MHz
VBW	OFF
SWT	20 ms
Sampling time T_s	12 µs

if we had used the same f_c, only traffic channels would have been captured by in measurements. RBW is smaller than the SSB's one and, in general, than the 5G signal's one. This may imply a reduction of the measured power, although it does not change the ratio between the control (i.e., SSB) and traffic (i.e., RB) channel contributions to the overall power given the deployment of the full downlink capacity: it will only operate as if the system has a smaller bandwidth with a smaller number of RBs. As for the VBW, the measurement instrument can not be set with a larger VBW than the RBW, which would be the ideal condition for noise-like signal measurement. We determined that the best condition is therefore to set VBW off.

3) A Keysight MXA N9020A Vector Signal Analyzer (VSA) connected to an R&S HL035 antenna was used to measure, after demodulating the 5G signal, the power of the PBCH-DMRS for RE, averaged over the six SSBs that make up the SSB burst. To ensure the correct demodulation, it is necessary to set the VSA according to the specific configuration of the 5G signal (namely, SSB numerology, frequency offset with respect to the signal center frequency, pattern, periodicity) transmitted by the MaMIMO. Details about the measurement procedure can be found in [32].

The traffic (i.e., the RBs) and the instantaneous transmitted power P_t were sampled at the MaMIMO antenna input every 1 s and 2 s, respectively, through a software provided by Huawei. It should be noted that, in standard measurement procedures, RB and P_t data are not extracted with the same time resolution. CP measurements, due to the SWT and Trace configuration shown in Tab. 3, return a value every 20 s.

To comply with the requirement that the full download capacity of the MaMIMO system is deployed, as explained in Sect. IV, two 5G phones have been placed in the proximity of the measurement point and configured with a continuous UDP data transmission. Preliminary tests have shown that using only one UE would not allow for a complete saturation of the RBs transmission capacity. The distance between the UEs and the receiving antenna was optimized to minimize the effect of the uplink transmission on channel power measurements.

VI. EXPERIMENTAL RESULTS

In this section we present the results of the experimental validation of the methodology, described in Sect. IV, to characterize the performance of a Power Lock (PL) feature fixing the averaging interval τ according to [17], i.e., $\tau = 6\,\text{min}$. We recall that the methodology relies on a black-box approach that does not require a preliminary knowledge of the operational principles and technical details of the PL.

The procedure implied by the characterization principles on which the methodology is based requires that we execute three tests, one for each operational condition (see Tab. 2). Measurements of P_t, CP and Resource Blocks (RBs) are shown in Fig. 6. As already explained in the description of the methodology, some *idle* time is required between tests to change the equipment settings, yet keeping the system alive. Measurements have been run continuously during tests and idle times, and also for some time before test 1 and after test 3.

A. FIXING OF P_0

P_0 is fixed with test no. 1 (label "P_0; PL_{off}" in Fig. 6) by forcing the MaMIMO system to transmit the maximum number of available RBs constantly thus keeping P_t as constant as possible. Such condition is not always met and RBs decrease randomly falling from the 217 to about 180 (see the bottom facet of the plot). If we focus on times before 10:34:17 (red dashed vertical line), we see that P_t doesn't seem to be very sensitive to such decrease, mostly because of the large dynamic of the logarithmic scale that doesn't allow to appreciate variations in the order of a few Watt at most. To better investigate this behavior, we compared P_t, CP and RB before and after 10:34:17 (see the white inset in Fig. 6) on a linear scale. Fig. 7 clearly shows

This article has been accepted for publication in a future issue of this journal, but has not been fully edited. Content may change prior to final publication. Citation information: DOI 10.1109/ACCESS.2020.3024764, IEEE Access

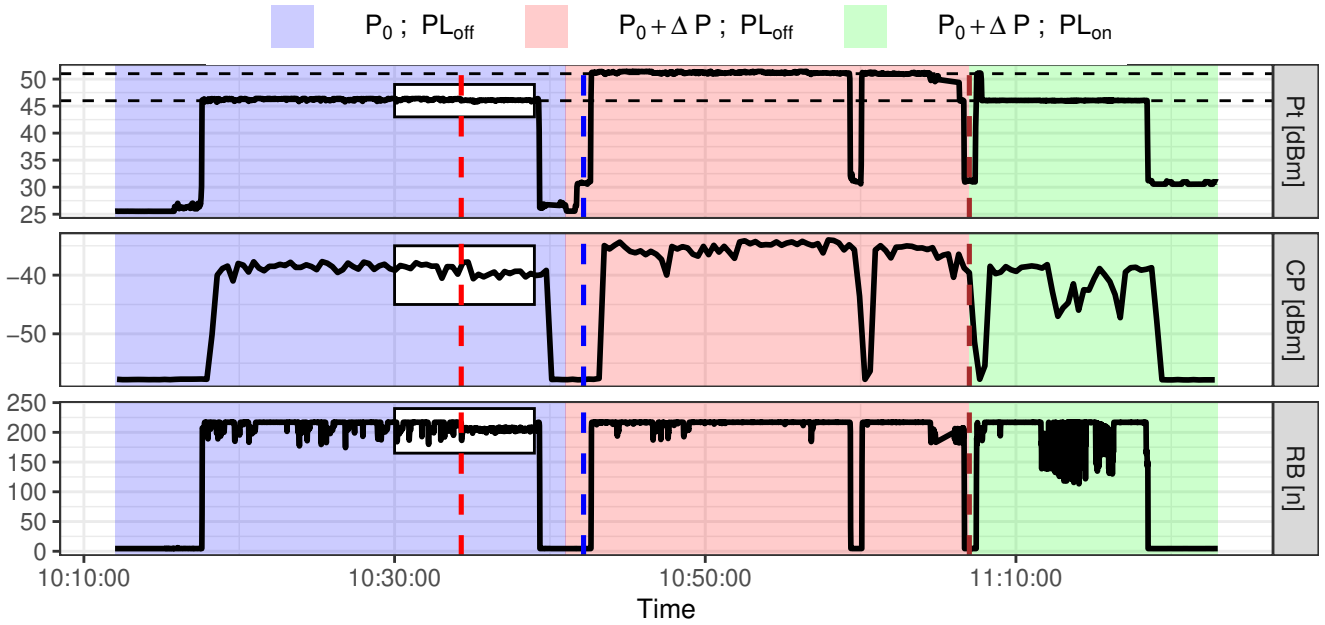

Figure 6. Power transmitted by the MaMIMO antenna (top trace), Channel Power (CP) measurements (middle trace) and transmitted Resource Blocks (RBs) (bottom trace).

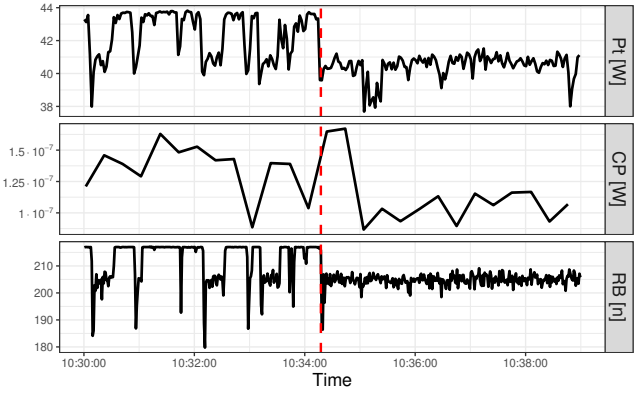

Figure 7. Time window of Fig. 6 in linear units.

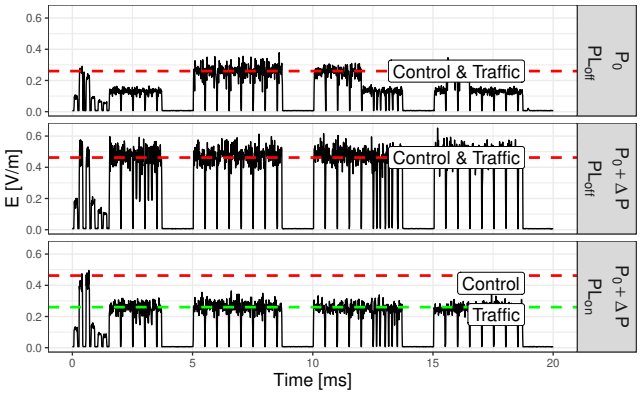

(a) E field strength.

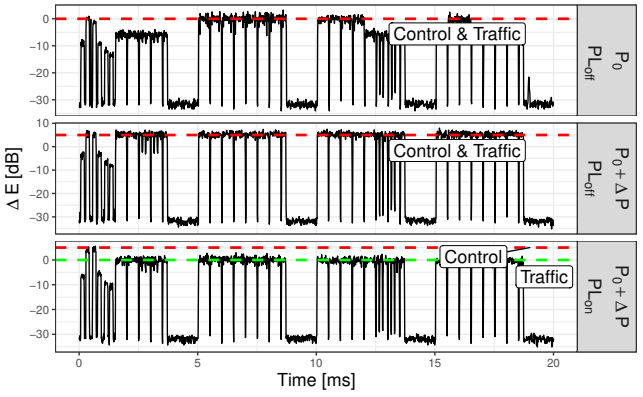

(b) E field strength relative to the reference configuration (P_0; $\mathrm{PL_{off}}$).

Figure 8. Zero Span E field strength.

that P_t follows RBs almost perfectly and that whenever a reduction in RB occurs it implies a reduction in P_t.

The same figure is also helpful to explain the behavior of CP measurements over time shown in Fig. 6: as expected, the radiated power that reaches measurement chain 2) described in Sect. V decreases with P_t. We wish to underline that CP is the average of 200 traces of 100 ms each and therefore its curve is smoothed and delayed with respect to P_t. At the end of the procedure, P_0 has been determined to be $P_0 = 44.7\,\mathrm{dBm}$, so that $P_{\max} = 46\,\mathrm{dBm}$ (see Tab. 2).

The top trace of Fig. 8a shows the EMF strength E over time once the value of P_0 has been assessed. The observation interval is 20 ms, i.e., the length of two frames. The first 5 ms are reserved to the transmission of the SSB burst. The trace shows that the maximum amplitude for

This article has been accepted for publication in a future issue of this journal, but has not been fully edited. Content may change prior to final publication. Citation information: DOI 10.1109/ACCESS.2020.3024764, IEEE Access

both traffic and control channels is $\hat{E} = 0.26\,\mathrm{V/m}$. This is only a fraction of E_0 that has been determined according to the restriction on human exposure explained in Sect. IV: namely, given that the RBW of the measurement chain 2) presented in Sect. V is only one fortieth of the 5G bandwidth, we have $\hat{E} = E_0/\sqrt{80/2} \simeq E_0/6.32\ \mathrm{V/m}$.

During this specific acquisition the UE the RBs fluctuated around the full downlink capacity: this is the reason why the traffic channels are not constant at $\hat{E}$.

Since this is the exposure condition that will be used as a reference for the validation of steps 2) and 3) of the methodology, in Fig. 8b we have reported the same quantities of Fig. 8a in logarithmic units, normalized to $\hat{E}$ obtained in step 1).

B. INCREASE OF P_{MAX}

Test no. 2 (label "$\mathrm{P_0} + \Delta\mathrm{P}; \mathrm{PL_{off}}$" in Fig. 6) shows what happens when $P_{\max}$ is increased by $\Delta P = 5\,\mathrm{dB}$ and PL is inactive (see Tab. 2). Exploiting the full download capacity by forcing the transmission of the maximum number of RBs, as shown in the bottom trace of Fig. 6, we see that the instantaneous power P_t increases by ΔP (see top trace) and the CP also increases, although the measured increment is slightly less than 5 dB that, however, is a plausible value given the 1.5 dB uncertainty ($k = 2$) for that measurement chain.

Because of the inactivity of PL, the E field increases to 0.46 V/m for both the traffic and control channels, as shown in the middle trace of Fig. 8a. Furthermore, the corresponding middle trace of Fig. 8b confirms that the increase has been of the same amount as $P_{\max}$, i.e., $\Delta E = 5\,\mathrm{dB}$. It is apparent that because of the increase of P_t and inactivity of PL $E > \hat{E}$.

By looking at the idle time between test no. 1 and 2 (see hours 10:42:10, blue dashed vertical line) we see an increase in P_t by ΔP even if there is no data transmission. This is because during that interval traffic channels are off, while control channels are active (i.e., SSBs are still transmitted) to keep the system alive and reachable by the UE. This will be discussed in details in Sect. VI-D, which discusses the behavior of the demodulated power of the PBCH-DMRS during both idle intervals and active transmission.

C. VALIDATION OF PL

The action of PL on P_t is tested with test no. 3 (label "$\mathrm{P_0} + \Delta\mathrm{P}; \mathrm{PL_{on}}$" in Fig. 6). We see that at the very beginning of the test, when data transmission occurs with the maximum RBs, P_t is transmitted at the same level as test no. 2, i.e., under condition $\mathrm{PL_{off}}$. This is because PL limits P_t so that the average value does not exceed P_0. Indeed, after a few seconds where $P_t = P_0 + \Delta P$, PL senses that P_0 is being approached and it limits P_t to $P_t = P_0$ without limiting the number of RBs. The PL adjusts the power of the PDSCH without reducing the assigned RBs.

Because of the 20 s averaging time, CP measurements do not follow the instantaneous variations of P_t and its level during the test goes to the same level of test no. 1.

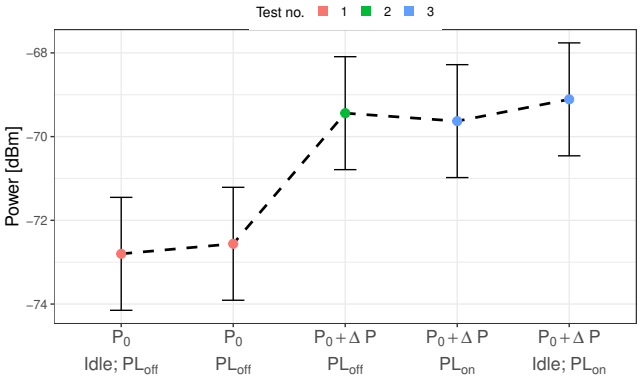

Figure 9. Demodulated power of the PBCH-DMRS.

The same figure shows that during the test there is a strong reduction in the number of RBs transmitted without a reduction of P_t. According to the manufacturer, this happens because the PL is interacting with the downlink scheduler in such a way that results in a reduction of the assigned RBs yet transmitting each RB at a higher power. Moreover, we can observe that the CP fluctuates in this period following the RBs. The explanation for this behavior has been provided by the system manufacturer that claimed that during that interval the MaMIMO antenna is performing a beam optimization, both in terms of power and RBs, and that the beam swings so that it is not always pointed toward the UEs.

The E field strength for this test is shown in the bottom trace of Fig. 8a, where we see that, thanks to the action of PL, traffic channels are clearly pushed down to the reference level $\hat{E}$ of test no. 1 while, as expected, the SSBs are affected by the ΔP increase and are therefore at $E = 0.46\,\mathrm{V/m}$. The 5 dB ratio between the traffic and control channel is apparent in the bottom row of Fig. 8b.

Note that PL is activated during the idle time between test no. 2 and 3, around hours 11:07:00 (brown dashed vertical line). We can see from Fig. 6 that P_t during that interval is the same as the one transmitted during idle time immediately before data transmission of test no. 2 and the one transmitted during a temporary data transmission switch off occurred during test no. 2. Again, this happens because during that time SSBs are active and transmitted at the maximum allowed power $P_{\max}$, which is now $P_{\max} = 51\,\mathrm{dBm}$.

D. PBCH-DMRS POWER

To further investigate the different effect of the PL on traffic and control channels, the demodulated power of the PBCH Demodulation Reference Signal (PBCH-DMRS) in each test condition is reported in Fig. 9.

We observe that the demodulated power in test no. 1 is similar for both *idle* and *active transmission* conditions. We also observe that for tests no. 2 and 3, both having $P_{\max} = P_0 + \Delta P = 51\,\mathrm{dBm}$, the measured power is comparable, and

that condition holds for both idle and active transmission. Since test no. 2 refers to PL_{off} and test no. 3 to PL_{on}, this confirms that the PL acts only on traffic and not on control channels transmitted in the SSBs.

Furthermore, even though the measured values do not differ by the increment $\Delta P = 5\,\mathrm{dB}$ applied to P_{max}, given that the uncertainty budget is $u = 1.35\,\mathrm{dB}$ ($k = 2$) and that, in turn, the distance between the lowest upper bound of the uncertainty intervals for $P_0 + \Delta P$ and the highest lower bound of the uncertainty intervals for P_0 is about 5.7 dB, we can still assume that ΔP is a plausible value for the increment in PBCH-DMRS power.

VII. CONCLUSIONS

In this paper we have proposed and validated a methodology to characterize an automatic tool (named Power Lock (PL)) designed for monitoring and controlling the average power transmitted by an MaMIMO antenna so that the exposure to electromagnetic fields generated by 5G systems, averaged over a reference interval, complies with exposure limits.

The methodology requires that the transmitted power and resulting EMF strength are monitored under three different conditions, thus the validation procedure requires three different steps to: 1) determine the average power P_0 that guarantees that the EMF exposure complies with the applicable limits; 2) increase the maximum power transmitted by the MaMIMO antenna and check that both control and traffic channels amplitude increases; 3) turn the PL feature on and verify that it limits the traffic channels power without affecting the control channels.

Experimental results proved that the proposed methodology matches the purposes and also allowed to gain insight into some other specific operational features of the PL. More specifically, results confirm the effectiveness of the methodology in demonstrating that the PL feature limits the average transmitted power of the traffic channels, regardless of the configured maximum power, without affecting the control channels, and that the EMF average exposure limit is not exceeded as well.

References

[1] J. G. Andrews, S. Buzzi, W. Choi, S. V. Hanly, A. Lozano, A. C. K. Soong, and J. C. Zhang, "What Will 5G Be?" *IEEE Journal on Selected Areas in Communications*, vol. 32, no. 6, pp. 1065–1082, 6 2014. [Online]. Available: http://ieeexplore.ieee.org/lpdocs/epic03/wrapper.htm?arnumber=6824752

[2] M. H. Alsharif and R. Nordin, "Evolution towards fifth generation (5G) wireless networks: Current trends and challenges in the deployment of millimetre wave, massive MIMO, and small cells," *Telecommunication Systems*, vol. 64, no. 4, pp. 617–637, 4 2017. [Online]. Available: http://link.springer.com/10.1007/s11235-016-0195-x

[3] D. Tse and P. Viswanath, *Fundamentals of Wireless Communication*. Cambridge University Press, 5 2005. [Online]. Available: https://www.cambridge.org/core/product/identifier/9780511807213/type/book

[4] E. Dahlman, S. Parkvall, and J. Sköld, *5G NR: The Next generation wireless Access technology*. Academic Press, 2018.

[5] S. Ahmadi, *5G NR: Architecture, Technology, Implementation, and Operation of 3GPP New Radio Standards*. Elsevier, 2019. [Online]. Available: https://linkinghub.elsevier.com/retrieve/pii/C20160049446

[6] T. L. Marzetta, G. Caire, M. Debbah, I. Chih-Lin, and S. K. Mohammed, "Special issue on Massive MIMO," *Journal of Communications and Networks*, vol. 15, no. 4, pp. 333–337, 8 2013. [Online]. Available: http://ieeexplore.ieee.org/document/6608229/

[7] E. G. Larsson, O. Edfors, F. Tufvesson, and T. L. Marzetta, "Massive MIMO for next generation wireless systems," *IEEE Communications Magazine*, vol. 52, no. 2, pp. 186–195, 2 2014. [Online]. Available: https://ieeexplore.ieee.org/document/6736761/

[8] L. Lu, G. Y. Li, A. L. Swindlehurst, A. Ashikhmin, and R. Zhang, "An Overview of Massive MIMO: Benefits and Challenges," *IEEE Journal of Selected Topics in Signal Processing*, vol. 8, no. 5, pp. 742–758, 10 2014. [Online]. Available: http://ieeexplore.ieee.org/document/6798744/

[9] T. L. Marzetta, "Massive MIMO: An Introduction," *Bell Labs Technical Journal*, vol. 20, pp. 11–22, 2015. [Online]. Available: http://ieeexplore.ieee.org/lpdocs/epic03/wrapper.htm?arnumber=7064850

[10] K. Zheng, S. Ou, and X. Yin, "Massive MIMO Channel Models: A Survey," *International Journal of Antennas and Propagation*, vol. 2014, pp. 1–10, 2014. [Online]. Available: http://www.hindawi.com/journals/ijap/2014/848071/

[11] X. Gao, O. Edfors, F. Rusek, and F. Tufvesson, "Massive MIMO Performance Evaluation Based on Measured Propagation Data," *IEEE Transactions on Wireless Communications*, vol. 14, no. 7, pp. 3899–3911, 7 2015. [Online]. Available: http://arxiv.org/abs/1403.3376http://dx.doi.org/10.1109/TWC.2015.2414413http://ieeexplore.ieee.org/document/7062910/

[12] F. W. Vook, A. Ghosh, and T. A. Thomas, "MIMO and beamforming solutions for 5G technology," in *2014 IEEE MTT-S International Microwave Symposium (IMS2014)*. IEEE, 6 2014, pp. 1–4. [Online]. Available: http://ieeexplore.ieee.org/document/6848613/

[13] B. Thors, A. Furuskar, D. Colombi, and C. Tornevik, "Time-Averaged Realistic Maximum Power Levels for the Assessment of Radio Frequency Exposure for 5G Radio Base Stations Using Massive MIMO," *IEEE Access*, vol. 5, pp. 19 711–19 719, 2017. [Online]. Available: http://ieeexplore.ieee.org/document/8039290/

[14] D. Colombi, P. Joshi, B. Xu, F. Ghasemifard, V. Narasaraju, and C. Törnevik, "Analysis of the Actual Power and EMF Exposure from Base Stations in a Commercial 5G Network," *Applied Sciences*, vol. 10, no. 15, p. 5280, 7 2020. [Online]. Available: https://www.mdpi.com/2076-3417/10/15/5280

[15] *Determination of RF field strength, power density and SAR in the vicinity of radiocommunication base stations for the purpose of evaluating human exposure*, IEC - International Electrotechnical Commission Std. IEC 62 232, 2017.

[16] International Electrotechnical Commission, "IEC-TR 62669 – Case studies supporting IEC 62232 - Determination of RF field strength, power density and SAR in the vicinity of radiocommunication base stations for the purpose of evaluating human exposure," IEC, Tech. Rep. IEC-TR 62669, 2019.

[17] A. Ahlbom, U. Bergqvist, J. Bernhardt, J. Cesarini, L. Court, M. Grandolfo, M. Hietanen, A. McKinlay, M. Repacholi, D. Sliney, J. Stolwijk, M. Swicord, L. Szabo, M. Taki, T. Tenforde, H. Jammet, and R. Matthes, "Guidelines for limiting exposure to time-varying electric, magnetic, and electromagnetic fields (up to 300 GHz)," *Health Physics*, vol. 74, no. 4, pp. 494–521, 1998.

[18] International Commission on Non-Ionizing Radiation Protection (ICNIRP), "Guidelines for Limiting Exposure to Electromagnetic Fields (100 kHz to 300 GHz)," *Health Phys.*, vol. 118, no. 5, pp. 483–524, may 2020.

[19] H. Keller, "On the Assessment of Human Exposure to Electromagnetic Fields Transmitted by 5G NR Base Stations," *Health Physics*, vol. 117, no. 5, pp. 541–545, 11 2019. [Online]. Available: http://journals.lww.com/00004032-201911000-00007

[20] NGMN Alliance. (2020, april) Recommendation on Base Station Active Antenna System Standards. [Online]. Available: https://www.ngmn.org/wp-content/uploads/Publications/2020/NGMN_BASTA-AA_WP_1_0.pdf

[21] D. Franci, S. Coltellacci, E. Grillo, S. Pavoncello, T. Aureli, R. Cintoli, and M. D. Migliore, "An Experimental Investigation on the Impact of Duplexing and Beamforming Techniques in Field Measurements of 5G Signals," *Electronics*, vol. 9, no. 2, p. 223, 1 2020. [Online]. Available: https://www.mdpi.com/2079-9292/9/2/223

[22] 3rd Generation Partnership Project (3GPP)". (2017) The 3GPP Specification 38 Series, document TS 38. [Online]. Available: https://www.3gpp.org/DynaReport/38-series.htm

[23] *NR; Physical channels and modulation*, 3rd Generation Partnership Project (3GPP) Std. Tech. Spec. 38.211, Rev. 15.1.0, april 2018.

[24] *NR; Physical layer procedures for control*, 3rd Generation Partnership Project (3GPP) Std. Tech. Spec. 38.213, Rev. 15.1.0, april 2018.
[25] Z. E. Ankarali, B. Pekoz, and H. Arslan, "Flexible Radio Access Beyond 5G: A Future Projection on Waveform, Numerology, and Frame Design Principles," *IEEE Access*, vol. 5, pp. 18 295–18 309, 2017. [Online]. Available: http://ieeexplore.ieee.org/document/7883931/
[26] A. Yazar and H. Arslan, "Flexible Multi-Numerology Systems for 5G New Radio," *Journal of Mobile Multimedia*, vol. 14, no. 4, pp. 367–394, 2018. [Online]. Available: http://www.riverpublishers.com/journal_read_html_article.php?j=JMM/14/4/2
[27] P. Guan, D. Wu, T. Tian, J. Zhou, X. Zhang, L. Gu, A. Benjebbour, M. Iwabuchi, and Y. Kishiyama, "5G Field Trials: OFDM-Based Waveforms and Mixed Numerologies," *IEEE Journal on Selected Areas in Communications*, vol. 35, no. 6, pp. 1234–1243, 6 2017. [Online]. Available: http://ieeexplore.ieee.org/document/7888960/
[28] M. Iwabuchi, A. Benjebbour, Y. Kishiyama, D. Wu, T. Tian, L. Gu, Y. Cui, and T. Kashima, "5G Field Experimental Trial on Frequency Domain Multiplexing of Mixed Numerology," in *2017 IEEE 85th Vehicular Technology Conference (VTC Spring)*. IEEE, 6 2017, pp. 1–5. [Online]. Available: http://ieeexplore.ieee.org/document/8108645/
[29] A. A. Zaidi, R. Baldemair, H. Tullberg, H. Bjorkegren, L. Sundstrom, J. Medbo, C. Kilinc, and I. Da Silva, "Waveform and Numerology to Support 5G Services and Requirements," *IEEE Communications Magazine*, vol. 54, no. 11, pp. 90–98, 11 2016. [Online]. Available: http://ieeexplore.ieee.org/document/7744816/
[30] L. Zhang, A. Ijaz, P. Xiao, A. Quddus, and R. Tafazolli, "Subband Filtered Multi-Carrier Systems for Multi-Service Wireless Communications," *IEEE Transactions on Wireless Communications*, vol. 16, no. 3, pp. 1893–1907, 3 2017. [Online]. Available: http://ieeexplore.ieee.org/document/7829438/
[31] A. Ijaz, L. Zhang, M. Grau, A. Mohamed, S. Vural, A. U. Quddus, M. A. Imran, C. H. Foh, and R. Tafazolli, "Enabling Massive IoT in 5G and Beyond Systems: PHY Radio Frame Design Considerations," *IEEE Access*, vol. 4, pp. 3322–3339, 2016. [Online]. Available: http://ieeexplore.ieee.org/document/7499809/
[32] S. Adda, T. Aureli, S. D'Elia, D. Franci, E. Grillo, M. D. Migliore, S. Pavoncello, F. Schettino, and R. Suman, "A Theoretical and Experimental Investigation on the Measurement of the Electromagnetic Field Level Radiated by 5G Base Stations," *IEEE Access*, vol. 8, pp. 101 448–101 463, 2020. [Online]. Available: https://ieeexplore.ieee.org/document/9103530/
[33] B. Xu, K. Zhao, B. Thors, D. Colombi, O. Lundberg, Z. Ying, and S. He, "Power Density Measurements at 15 GHz for RF EMF Compliance Assessments of 5G User Equipment," *IEEE Transactions on Antennas and Propagation*, vol. 65, no. 12, pp. 6584–6595, 2017.
[34] R. Pawlak, P. Krawiec, and J. Zurek, "On Measuring Electromagnetic Fields in 5G Technology," *IEEE Access*, vol. 7, pp. 29 826–29 835, 2019. [Online]. Available: https://ieeexplore.ieee.org/document/8660395/
[35] S. Aerts, L. Verloock, M. Van Den Bossche, D. Colombi, L. Martens, C. Tornevik, and W. Joseph, "In-situ Measurement Methodology for the Assessment of 5G NR Massive MIMO Base Station Exposure at Sub-6 GHz Frequencies," *IEEE Access*, vol. 7, pp. 184 658–184 667, 2019. [Online]. Available: https://ieeexplore.ieee.org/document/8937514/
[36] D. Franci, S. Coltellacci, E. Grillo, S. Pavoncello, T. Aureli, R. Cintoli, and M. D. Migliore, "Experimental Procedure for Fifth Generation (5G) Electromagnetic Field (EMF) Measurement and Maximum Power Extrapolation for Human Exposure Assessment," *Environments*, vol. 7, no. 3, p. 22, 3 2020. [Online]. Available: https://www.mdpi.com/2076-3298/7/3/22

SARA ADDA received the M.Sc. (cum laude) degree in physics and the postgraduate specialization degree in health physics from Turin University, Italy, in 1998 and 2003 respectively. She worked for one year (1998-1999) at ENEA Casaccia (Rome) within the Interdepartmental Computing and High Performance Networks Project, implementing a system for the simulation of electromagnetic field dynamics in complex environments through the use of massively parallel architectures.

Since 1999 she has been working in ARPA Piedmont, in the Physical and Technological Risk Department, dealing with control and monitoring of non-ionizing radiation and the development of theoretical forecasting/numerical calculation methods, both in the low and high frequency ranges. She also participates in the CEI (Italian Electrotechnical Committee) working groups, for the drafting of technical standards on measurement and evaluation methods for human emf exposure, and she deals with the theoretical and practical aspects related to the measurement of electromagnetic fields in the workplace. In this context, she is the representative of the Piedmont Region in the interregional technical coordination group. She participates in European (Twinning Italy-Poland project) and international collaborative projects (Arpa Piemonte - Beijing Municipal Environmental Protection Bureau), on methods and techniques for measuring and evaluating human exposure to emf both in the workplace and in the living environment.

TOMMASO AURELI received the M.Sc. degree in biological science in 1985 from Sapienza University, Rome, Italy, in 1985. He joined ARPA Lazio in 2002. From 2004 to 2018, he was director of the EMF divison, being involved in both measurement and previsional evaluation of EMF from civil sources. He is currently director of the Department of Rome.

STEFANO COLTELLACCI received the M.Sc. degree in Aerospace Engineering from the Sapienza University of Rome. He works as consultant for various Italian space sector companies involved in ESA, ASI and IT MoD missions and projects for EO, space exploration and satellite constellations for telecommunication in system engineering tasks. In 2005 joined Agenzia Regionale della Protezione Ambientale del Lazio (environmental agency of the Lazio Region, ARPA Lazio), he worked in Air Quality, Ionizing Radiation and RF sectors. Since 2011 works in the the prevention and monitoring of electromagnetic pollution group of ARPA Lazio local Department of Rome, supporting activities in RF measurements, collaborations with other Italian Environmental Regional Agencies and Government organizations.

This article has been accepted for publication in a future issue of this journal, but has not been fully edited. Content may change prior to final publication. Citation information: DOI 10.1109/ACCESS.2020.3024764, IEEE Access

STEFANO D'ELIA received his M.Sc. (*magna cum laude*) in Electronics Engineering in 1997 from the University of Rome "La Sapienza".

He joined Vodafone Italy (formerly Omnitel) in 1998, where he is currently covering the role of Mobile Access Integrated Solutions Manager in Vodafone Group Network, based in Ivrea (Turin), Italy. In 2012 he was awarded as a Vodafone Distinguished Engineer, one of the highest steps in the technical career path at Vodafone. His main professional interests are energy efficiency modeling for mobile networks, and calculation and measurements for the assessment of human exposure to high-frequency electromagnetic fields from mobile base stations.

He has been national delegate in several standard bodies on electromagnetic fields measurements and calculations, and since 2002 he is the appointed chairman of the Working Group "Mobile Base Stations" within the Technical Committee 106 "Human exposure to electromagnetic fields" of the Italian Electrotechnical Committee.

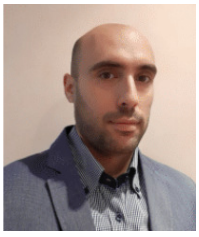

DANIELE FRANCI received the M.Sc. degree (*magna cum laude*) and the Ph.D. degree in nuclear and subnuclear physics from Sapienza University, Rome, Italy, in 2007 and 2011 respectively. From 2009 to 2011, he was an Analyst Technologist with the Nucleco SPA involved in radiological characterization of radioactive wastes from the decommissioning of former Italian nuclear power plants. He joined ARPA Lazio in 2011, being involved in RF EMF human exposure assessment. Since 2017 he has been involved in activities of CEI for the definition of technical procedures for EMF measurement from 4G/5G MIMO sources.

ENRICO GRILLO received the M.Sc. degree in electronics engineering from the Seconda Università di Napoli in 1999, Aversa, Italy. In 2000 he works as RF to grow up the first 3G telecommunication radio Network. Since 2005 he is involved as research technician in prevention and monitoring of electromagnetic pollution at ARPA Lazio, the local environmental agency of the Lazio Region.

NICOLA PASQUINO (AM'99–M'02–SM'13) was born in Naples, Italy in 1973. He received his M.Sc. (*magna cum laude*) in Electronics Engineering in 1998 and his Ph.D. in Information Engineering in 2002, both from the Università degli Studi di Napoli Federico II, Naples, Italy.

He is an Associate Professor of Electrical and Electronic Measurements at the Università degli Studi di Napoli Federico II, Naples, Italy. His research interests are in the field of electromagnetic compatibility measurements and measurements of human exposure to high-frequency electromagnetic fields, with application of machine learning methodologies to measurement data analysis. He is the Chief Scientist at the Electromagnetic Compatibility Laboratory of his Department and President of the TC106 "Human exposure to electromagnetic fields" of the Italian Electrotechnical Committee. He serves as an Editor for the Journal of Electrical and Computer Engineering, as a Section Editor for the Acta IMEKO journal and is a member of the Editorial Board for the Measurement Science Review journal.

Prof. Pasquino has been awarded a Fulbright Scholarship at the University of Pennsylvania, Philadelphia PA, USA. He's been a member of Rotary since 2005 and has been President of Rotary Club Napoli Angioino in 2019-2020.

SETTIMIO PAVONCELLO was born in Rome, Italy in 1973. He received the M.Sc. degree in telecommunication engineering from Sapienza University of Rome, Italy, in 2001. Since 2002, he has been working for Regional Environmental Agency of Lazio in Rome EMF Department. He is specialized in electromagnetic field measurements and EMF projects evaluation related to radio, TV and mobile communications systems maturing huge experience in the use of broadband and selective instruments. In last years he has deepened the issues related to measurements on LTE and NB-IoT signals. Since 2018 he has been actively involved in the Working Group "Mobile Base Stations" within the Technical Committee 106 of the Italian Electrotechnical Committee (CEI) aimed at defining measurement procedures for mobile communications signals and is currently engaged in various projects concerning measurement on 5G signals.

RICCARDO SUMAN was born in Ivrea, Italy, in 1974. He received the BSc. degree in telecommunication engineering from Politecnico di Torino, Italy, in 1996. Since 1996, he has been with Vodafone Italy (formerly Omnitel Pronto Italia) where is currently working as antenna matter expert. He also participates to the BASTA AA (Recommendation on Base Station Active Antenna Standards) by NGMN Alliance. Since 2012, he has been involved in activities related to EMF focusing on measuring and modeling electromagnetic fields and electromagnetic exposure assessment of base stations for mobile communications. He also participates to the Technical Committee 106 of the Italian Electro Technical Committee (CEI) and as national delegate to the IEC TC106.

MATTIA VACCARONO was born in Ivrea, Italy, in 1990. He received the M.Sc. (magna cum laude) in Physics from Turin University in 2015. Since 2016, he has been working in the Regional Agency for Environmental Protection (Arpa Piemonte) of Piedmont region, Italy. He is specialized in EMF measurements and project assessments. He is currently enrolled in Colorado State University, Electrical and Computer Engineering Department, as PhD student, conducting research on weather radars and EMF interferences.